

MDPI

Article

Identification of a Novel Gene *MtbZIP60* as a Negative Regulator of Leaf Senescence through Transcriptome Analysis in *Medicago truncatula*

Jiayu Xing ¹, Jialan Wang ¹, Jianuo Cao ¹, Ke Li ¹, Xiao Meng ¹, Jiangqi Wen ², Kirankumar S. Mysore ³, Geng Wang ¹, Chunjiang Zhou ^{1,*} and Pengcheng Yin ^{1,*}

- Ministry of Education Key Laboratory of Molecular and Cellular Biology, Hebei Research Center of the Basic Discipline of Cell Biology, Hebei Collaboration Innovation Center for Cell Signaling and Environmental Adaptation, Hebei Key Laboratory of Molecular and Cellular Biology, College of Life Sciences, Hebei Normal University, Shijiazhuang 050024, China; 15097315361@163.com (J.X.); wangjialan0312@163.com (J.W.); c13082348698@163.com (J.C.); like@hebtu.edu.cn (K.L.); mengxiao2012@163.com (X.M.); gengwang@hebtu.edu.cn (G.W.)
- Department of Plant and Soil Sciences, Institute for Agricultural Biosciences, Oklahoma State University, Ardmore, OK 73401, USA; jiangqi.wen@okstate.edu
- Department of Biochemistry and Molecular Biology, Institute for Agricultural Biosciences, Oklahoma State University, Ardmore, OK 73401, USA; kmysore@okstate.edu
- * Correspondence: cjzhou@hebtu.edu.cn (C.Z.); yinpengcheng@hebtu.edu.cn (P.Y.); Tel.: +86-0311-80789671 (C.Z.); +86-0311-80787527 (P.Y.)

Abstract: Leaves are the primary harvest portion in forage crops such as alfalfa (*Medicago sativa*). Delaying leaf senescence is an effective strategy to improve forage biomass production and quality. In this study, we employed transcriptome sequencing to analyze the transcriptional changes and identify key senescence-associated genes under age-dependent leaf senescence in Medicago truncatula, a legume forage model plant. Through comparing the obtained expression data at different time points, we obtained 1057 differentially expressed genes, with 108 consistently up-regulated genes across leaf growth and senescence. Gene Ontology and Kyoto Encyclopedia of Genes and Genomes pathway enrichment analyses showed that the 108 SAGs mainly related to protein processing, nitrogen metabolism, amino acid metabolism, RNA degradation and plant hormone signal transduction. Among the 108 SAGs, seven transcription factors were identified in which a novel bZIP transcription factor MtbZIP60 was proved to inhibit leaf senescence. MtbZIP60 encodes a nuclear-localized protein and possesses transactivation activity. Further study demonstrated MtbZIP60 could associate with MtWRKY40, both of which exhibited an up-regulated expression pattern during leaf senescence, indicating their crucial roles in the regulation of leaf senescence. Our findings help elucidate the molecular mechanisms of leaf senescence in M. truncatula and provide candidates for the genetic improvement of forage crops, with a focus on regulating leaf senescence.

Keywords: leaf senescence; Medicago truncatula; transcriptome analysis; bZIP; WRKY



Citation: Xing, J.; Wang, J.; Cao, J.; Li, K.; Meng, X.; Wen, J.; Mysore, K.S.; Wang, G.; Zhou, C.; Yin, P. Identification of a Novel Gene *MtbZIP60* as a Negative Regulator of Leaf Senescence through Transcriptome Analysis in *Medicago truncatula*. *Int. J. Mol. Sci.* 2024, 25, 10410. https://doi.org/10.3390/ijms251910410

Academic Editor: Abir U. Igamberdiev

Received: 3 September 2024 Revised: 24 September 2024 Accepted: 25 September 2024 Published: 27 September 2024



Copyright: © 2024 by the authors. Licensee MDPI, Basel, Switzerland. This article is an open access article distributed under the terms and conditions of the Creative Commons Attribution (CC BY) license (https://creativecommons.org/licenses/by/4.0/).

1. Introduction

Leaf senescence represents the concluding stage of leaf development and is characterized by a transition from metabolism to catabolism. This stage involves the breakdown of organelles like chloroplasts, along with the degradation of biological macromolecule such as nucleic acids, proteins and lipids. The released organic and inorganic nutrients are then allocated to young leaves, developing flowers, seeds or other storage organs within the same plant, which is critical for its adaptability and reproductivity [1,2].

Leaf senescence is a crucial issue in both development biology and agronomy. In crop production, precocious leaf senescence can impact photosynthesis and impede grain filling, resulting in significant yield loss. Conversely, delaying leaf senescence may improve

final yield in specific scenarios [3–6]. It is estimated that postponing the senescence of functional leaves for one day can boost the yield of maize, rice, wheat and other crops by a range of 2–10% [7]. When it comes to forage crops, where leaves are primarily harvested, leaf senescence has a more obvious impact on the biomass yield and forage quality [8]. Therefore, revealing the molecular mechanism of leaf senescence can not only improve the comprehension of this fundamental biological process, but may also provide potential strategies for manipulation of leaf senescence, ultimately benefit crop production.

The initiation and progression of leaf senescence are not passive occurrences, but rather tightly controlled by different regulatory factors at multiple levels, including chromatin remodeling, transcription regulation, post-transcriptional regulation, translation regulation and post-translational regulation [1,9,10]. The onset of leaf senescence is basically determined by age. However, as senescence advances, a combination of extrinsic and intrinsic signals are incorporated into age information to regulate the senescence progression. These factors include nutritional and water status, hormone signals, light and temperature conditions and various biotic stresses. As a result, highly complex regulatory networks and multiple layers of regulatory pathways are interconnected to orchestrate the dynamic process of leaf senescence.

During the process of leaf senescence, leaves experience systematic physiological and biochemical changes, accompanied by alterations in gene expression. Genes that show increased expression are commonly referred to as senescence-associated genes (SAGs), while genes with decreased expression are known as senescence down-regulated genes (SDGs) [11,12]. The expression changes of numerous SAGs and SDGs contribute to the precise regulation of leaf senescence. Within the wide array of genes associated with senescence, the dynamic activation of transcription factors (TFs) is one of the hallmarks of leaf senescence [13,14]. These TFs present in multiple gene families, including NAC, WRKY, AP2/ERF, MYB, bZIP and bHLH, among which NAC and WRKY TFs have been widely studied and demonstrated to be essential in regulating senescence in different species [13,15–18]. NAC TFs plays both positive and negative roles in this process. In Arabidopsis, positive NAC regulators consist of ANAC082/ATAF1, ANAC016, ANAC019, ANAC028/AtNAP, ANAC032, ANAC046, ANAC055, ANAC059/ORS1, ANAC072, ANAC087 and ANAC092/ORE1 [19-27]. Intriguingly, only a limited number of NAC TFs exhibit negative regulatory functions, such as ANAC017, ANAC042/JUB1, ANAC075, ANAC082, ANAC083/VNI2, and ANAC090 [28–31]. WRKY family proteins are also one of the largest plant-specific TFs, characteristic for their invariant WRKYGQK motif [32]. It has been validated that WRKY6, WRKY22, WRKY26, WRKY42, WRKY45, WRKY53, WRKY54, WRKY55, WRKY70, WRKY71, and WRKY75 play vital roles in regulating leaf senescence in Arabidopsis, with WRKY54 and WRKY70 function as negative regulators [16,33–40].

Aside from NAC and WRKY, additional TFs such as the basic leucine zipper (bZIP) family, characterized by an alkaline region and a varied leucine zipper domain, also play an important role in the regulation of leaf senescence. However, only a small number of bZIP TFs have been found to be involved in regulation of leaf senescence. The bZIP TF G-box-binding factor 1 (GBF1/bZIP41), can bind to the G-boxes of the CATALASE2 and RBCS1a promoter to inhibit their transcription, thereby triggering the initiation of leaf senescence [41]. ABA (abscisic acid)-responsive element (ABRE) binding factors/ABREbinding proteins (ABFs/AREBs) ABF2, ABF3, ABF4 can directly bind to the promoter of Chlorophyll catabolic enzyme gene NYE1, NYE2, PAO, and NYC1 to activate their transcription, thus promoting ABA-induced leaf senescence in Arabidopsis [42]. A recent study found that ABF2/3/4 could bind and transactivate the expression of the kinase kinase kinase 18 (MAPKKK18) coding gene, mediating ABA facilitated leaf senescence [43]. ABF3 and ABF4 can also activate the transcription of NAC TFs, such as ANAC072, ANAC055 and ANAC019, to promote leaf senescence, indicating that various transcriptional regulatory pathways are interconnected through complex and robust networks, allowing for finetuning of leaf senescence [44,45]. Further study on bZIP TFs associated with senescence

could help shed light on the transcriptional regulatory mechanism underpinning leaf senescence regulation.

In the last few decades, there has been considerable advancement in elucidating the mechanism of leaf senescence in *Arabidopsis*, rice, wheat, tobacco and other species [15,17,46,47]. However, few studies have focused on the regulation of leaf senescence in legume forage. Alfalfa (*Medicago sativa*) is one of the most widely distributed forage legumes in the world because of its high yields, resistance, nutritional quality and adaptability [48–50]. At the same time, alfalfa has the characteristics of allogamy, self-incompatibly and autotetraploidy with a complex genetic background, impeding attempts to decipher the molecular principles of leaf senescence. Therefore, only a limit number of genes have been demonstrated to participate in leaf senescence regulation in alfalfa. For example, studies showed that alfalfa plants overexpressing the cytokinin biosynthetic gene *IPT* driven by the *SAG12* promoter, as well as those with a silenced chlorophyll catabolic gene which has been named STAY-GREEN (*SGR*) or overexpression of the γ -tocopherol methyltransferase gene *MsTMT*, exhibited a delayed leaf senescence phenotype, which could potentially improve the quantity and quality of forage [51–53]. In contrast, overexpressing *MsSAG113* could accelerate leaf senescence, indicating its crucial role in leaf senescence [54].

M. truncatula, a close relative of alfalfa, has been established as an appropriate model for genetic improvement and investigation of leaf senescence in forage crops due to its short growth period, self-pollination, small genome and high transformation efficiency [8,53,55,56]. Therefore, uncovering the molecular mechanism of leaf senescence in *M. truncatula* is of great theoretical and practical value for breeding high-yield varieties of alfalfa and other legume forage.

In order to determine the key regulators of leaf senescence, we employed a comparative transcriptome analysis over a time course, including young leaf, mature leaf and senescent leaf in *M. truncatula*. Further, we examined the detail expression profiles of leaf senescence and identified a novel bZIP TF MtbZIP60 that functions as a negative regulator of leaf senescence. This work will help to clarify the molecular regulatory mechanism underpinning leaf senescence in *M. truncatula* and provide a valuable gene resource for improving biomass yield and quality of legume forage.

2. Results

2.1. Changes in Physiological and Molecular Parameters during Age-Dependent Leaf Senescence

In order to comprehensively characterize the process of leaf senescence, we dynamically monitored the growth and senescence progression of M. truncatula ecotype R108 leaves. The content of chlorophyll and malondiadehyde (MDA) which are commonly used as indicators for the progression of leaf senescence were also detected at the same time, along with the expression of the senescence marker genes. For the purpose of consistency, the fifth and sixth compound leaf were utilized for investigation and subsequent transcriptome sequencing, and the day when the compound leaf was visible is considered as the first day. As illustrated in Figure 1, the expansion of leaves occurred at 5 d, reaching fully maturity at 15 d and senescence initiating at 30 d. Yellowing at the leaf tips became visible at 45 d, completely yellowing at 60 d and culminating with leaves falling (Figure 1A). The chlorophyll content rose from 3 d to 15 d, peaked at 15 d and then decreased (Figure 1B). The malondialdehyde (MDA) content displayed an intricate pattern throughout the process of leaf senescence. The MDA level remained consistent at 3 d and 5 d, experienced a slight decrease at 15 d, followed by an increase at 30 d and reached a maximum at 45 d and 60 d (Figure 1C). The expression of senescence up-regulated gene MtORE1, which is homologous to Arabidopsis ANAC092/ORE1, encoding a senescence-associated NAC TF, and senescence down-regulated gene MtCAB1, which is homologous to Arabidopsis CAB1, encoding a subunit of light-harvesting complex II, changed correspondingly accompanied by leaf senescence (Figure 1D,E). Based on the results of phenotypic analysis and physiological data, we selected the leaves at 5 d, 30 d and 60 d, which represented young leaf, mature leaf and senescent leaf, respectively, to perform transcriptome sequencing.

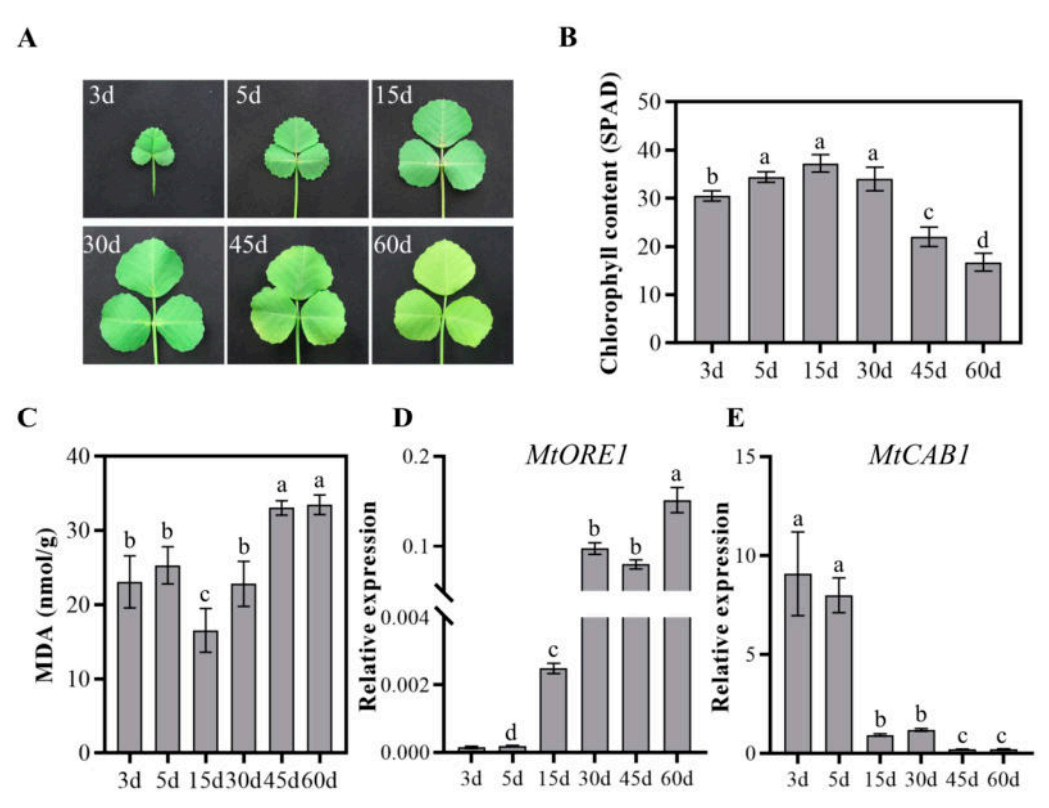


Figure 1. Physiological and biochemical analysis of leaf growth and senescence in *Medicago truncatula*. (**A**) Phenotype of the fifth compound leaf at different growth and senescence stages. The day when the fifth compound leaf emerged is considered as day 1. (**B**) Chlorophyll content in the fifth compound leaf at 3 d, 5 d, 15 d, 30 d, 45 d and 60 d. The chlorophyll content was obtained by measuring the SPAD value using a chlorophyll meter. Date is shown as mean \pm SD (n = 4). Significant differences revealed by Tukey's multiple comparison test are indicated by letters above bars (p < 0.05). (**C**) MDA content was measured in the fifth compound leaf at indicated time points. Date is shown as mean \pm SD (n = 4). Significant differences revealed by Tukey's multiple comparison test are indicated by letters above bars (p < 0.05). (**D**,**E**) Expression of senescence up-regulated and down-regulated marker genes MtORE1 (**D**) and MtCAB1 (**E**) at 3 d, 5 d, 15 d, 30 d, 45 d and 60 d. Date is shown as mean \pm SD (n = 3). Significant differences revealed by Tukey's multiple comparison test are indicated by letters above bars (p < 0.05).

2.2. Transcriptome Sequencing

Leaf samples at 5 d, 30 d and 60 d were harvested and subjected to transcriptome sequencing with three biological replicates at each point. A total of 54.79 Gb of clean data was collected, with each sample producing more than 5.75 Gb of data. The percentage of bases with a Phred value \geq 30% (Q30) exceeded 89.74%, and the alignment efficiency of clean reads with the reference genome varied from 80.47% to 88.39% (Table S7).

Principal component analysis (PCA) showed that the biological replicates from the same time point clustered together, indicating a significant level of similarity within the group. Across different stages of leaf senescence, the obtained transcriptomic data varied substantially, suggesting a higher degree of variability among different groups (Figure 2A). Additionally, the correlation between biological replicates was assessed using the Pearson correlation coefficient (PCC) analysis. The results revealed that all correlation coefficients between different samples within the same group exceeded 0.83, demonstrating a high level of consistency among the biological replicates (Figure 2B).

Int. J. Mol. Sci. 2024, 25, 10410 5 of 19

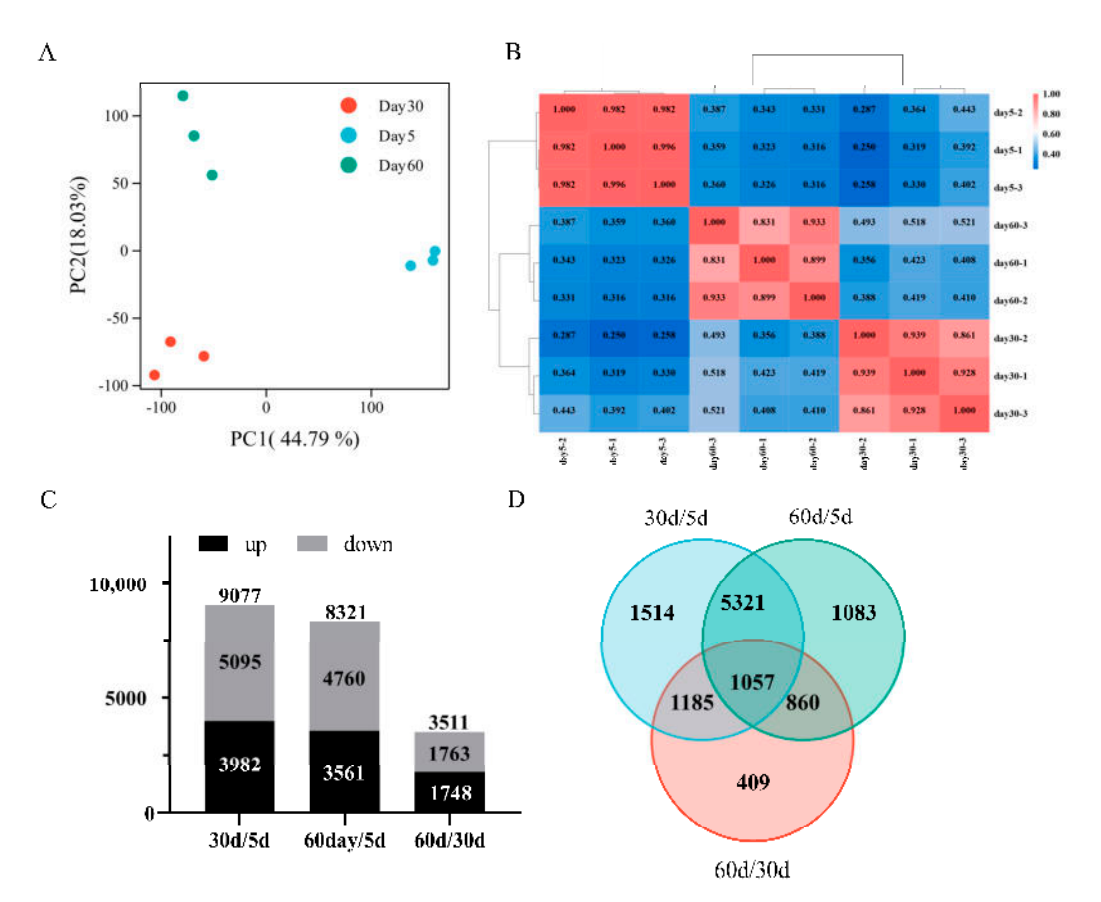


Figure 2. Transcriptomic overview of age-dependent leaf senescence in *Medicago truncatula*. (**A**) Principal component analysis (PCA) plot of transcriptome data from different leaf growth and senescence stages; (**B**) Pearson correlation coefficient of transcriptome profiles from different leaf growth and senescence stages; (**C**) The number of differentially expressed genes (DEGs) identified from various comparison combination, as determined based on FPKM values using DESeq2 with adjusted p-value < 0.01 and $|\log_2|$ (fold change) |>1| or $|\log_2|$ (D) Venn diagram of overlap DEGs among different comparisons.

Using DESeq2 with screening criteria of adjusted p-value < 0.01 and \log_2 (fold change) > 1 or <-1, the differentially expressed genes (DEGs) were identified in each group compared with one another (Table S2). A comparation between 30 d and 5 d revealed a total of 9077 DEGs, consisting of 5095 down-regulated genes and 3982 up-regulated genes. A comparable number of DEGs was obtained between 60 d versus 5 d, with a total of 8321 DEGs, including 4760 down-regulated genes and 3562 up-regulated genes. Fewer DEGs were identified between 60 d versus 30 d, totaling 3511 DEGs, with 1763 down-regulated genes and 1748 up-regulated genes, suggesting a similar gene expression profile between 60 d and 30 d (Figure 2C). Following a comparative analysis of DEGs obtained from different combinations, it was found that 1057 DEGs were shared among the comparison (Figure 2D).

2.3. Validation of Transcriptome Data by qRT-PCR

In order to confirm the accuracy of RNA-seq results, quantitative real-time PCR (qRT-PCR) was performed on selected genes exhibiting different expression patterns in a biological independent experiment. A total of twelve candidate genes were selected, categorized into four distinct expression profiles: continuous up-regulation genes, continuous down-regulation genes, genes that were up-regulated at 30 d and then down-regulated at 60 d and genes that were down-regulated at 30 d, then up-regulated at 60 d. The results showed that the expression of the specific gene in RNA-seq was consistent with the one detected in qRT-PCR (Figure 3). The Pearson correlation coefficient was calculated by

SPSS 17.0 software to evaluate the correlation between different detection methods. Overall, the results obtained from qRT-PCR were in line with the RNA-seq data, showing a correlation coefficient exceeding 0.82 (Figure 3). Thus, our data demonstrates the reliability and consistency of transcriptome analysis, which can be utilized for further investigating genes related to leaf senescence regulation in *M. truncatula*.

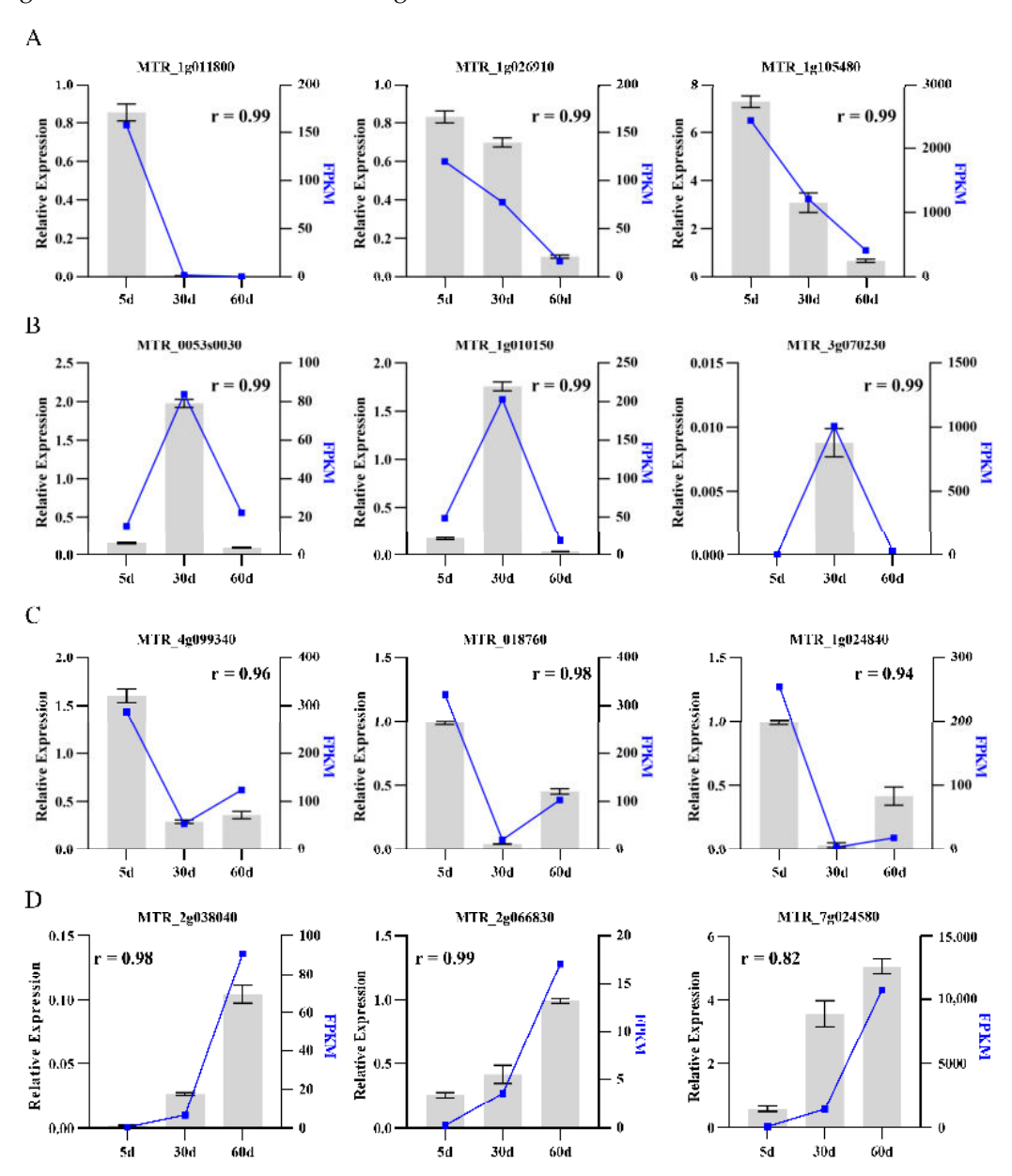


Figure 3. (**A–D**) Validation of selected transcripts by qRT-PCR. The expression of the specific gene in RNA-seq was represented by the lines on the right y-axis, whereas the relative expression of the same gene detected by qRT-PCR from independent replicates was depicted by the columns on the left y-axis. Date is shown as mean \pm SD (n = 3).

2.4. Short Time-Series Expression Miner (STEM) Clustering of DEGs during Leaf Growth and Senescence

In order to cluster and compare the obtained DEGs at different time points, we used Short Time-series Expression Miner (STEM) to identify the predominant model temporal expression profiles. Four significant and distinct expression profiles were identified, comprising three up-regulated profiles (14, 11 and 8) and one down-regulated profile (1) (Figure 4). Each profile consisted of a set of genes with a similar expression pattern.

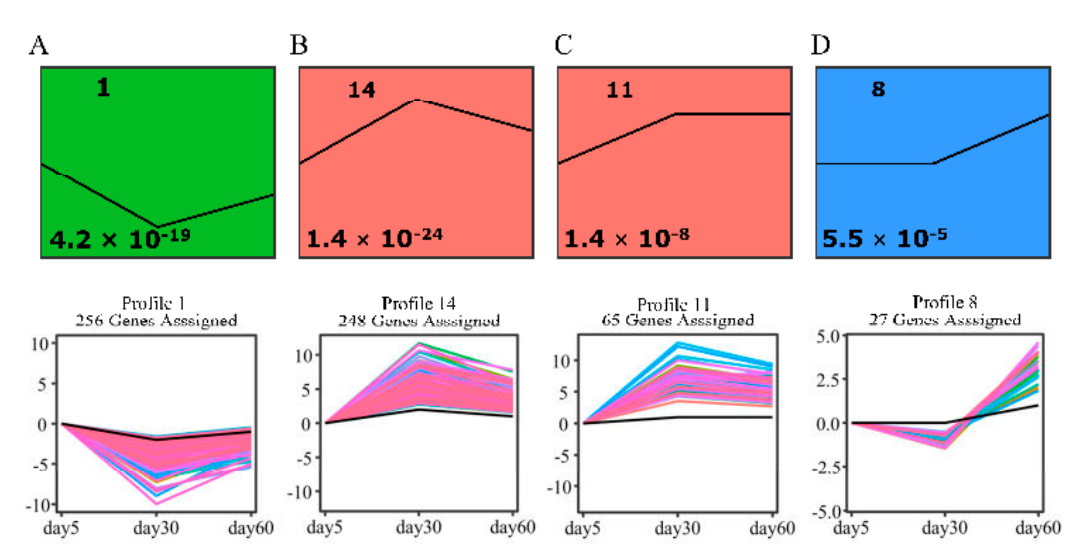


Figure 4. Short Time-series Expression Miner (STEM) clustering of 1057 DEGs shared by the three time points. (**A–D**) indicate different types of model expression profile, with the model profile ID number on the top left-hand corner and p-value on the bottom left. Different colors represent different significance. Only the model temporal expression profiles that has a significant number of assigned genes compared to the number of expected genes, with a p-value < 0.05, are displayed.

2.5. Gene Ontology Enrichment and Kyoto Encyclopedia of Genes and Genomes Pathway Enrichment Analysis of Senescence-Associated Genes

To further identify genes associated with leaf senescence, Venn diagrams based on upregulated DEGs obtained from comparisons between different time points were generated. A total of 108 *SAGs* shared by the three time points were detected (Figure 5A; Table S3). Then, we performed GO enrichment analysis to characterize the gene function of the 108 *SAGs*. The analysis classified the gene function into three categories, including biological process, molecular function and cellular component. Specifically, the "cellular process", "metabolic process", "single-organism process", "biological regulation" and "localization" were the main enriched terms in the biological process category. Significant enriched terms in the cellular component category included "cell", "cell part", "membrane", "organelle", "membrane part" and "organelle part". In the molecular function category, enriched terms were "binding", "catalytic activity", "transporter activity" and "nucleic acid binding transcription factor activity" (Figure 5B; Table S4).

Kyoto Encyclopedia of Genes and Genomes (KEGG) pathway enrichment analysis showed that the significant enriched pathway in the 108 *SAGs* were "endocytosis", "indole alkaloid biosynthesis", "spliceosome", "protein processing in endoplasmic reticulum", "nitrogen metabolism", "beta-Alanine metabolism", "alpha-Linolenic acid metabolism" and "RNA degradation" (Figure 5C; Table S4).

2.6. Comparison of Senescence-Associated Genes between Medicago and Arabidopsis

As significant advancement had been made in understanding the molecular mechanism of leaf senescence in *Arabidopsis*, we compared the identified *SAGs* with homologous genes in *Arabidopsis* and analyzed their putative function in leaf senescence regulation using the leaf senescence database (LSD 5.0, https://ngdc.cncb.ac.cn/lsd/index.php (accessed on 1 May 2024)). In *Arabidopsis*, 92 out of 108 homologous genes are documented in the LSD database (Supplemental Table S5). Notably, there are six genes in *Arabidopsis* known to play a role in senescence regulation, including *RD29B*, *SAUR72*, *AGL8*, *PYL5*, *WRKY71* and *LOX1* (Table 1). Additionally, two genes in *Arabidopsis* serve as marker genes for leaf senescence (Table 1). These findings confirm the validity of the experimental design and the accuracy of sampling timing.

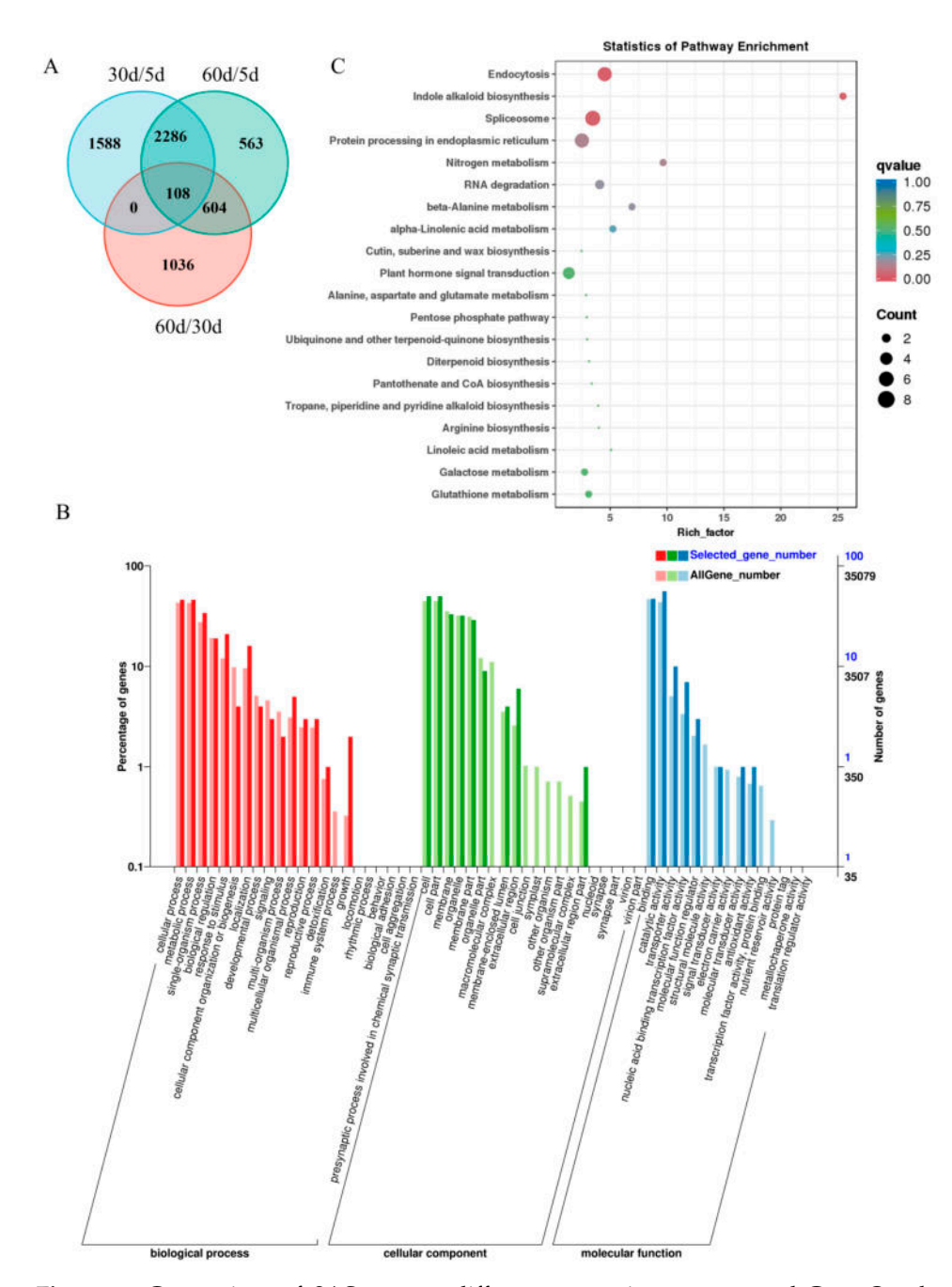


Figure 5. Comparison of *SAGs* among different comparison groups and Gene Ontology (GO) enrichment and Kyoto Encyclopedia of Genes and Genomes (KEGG) enrichment analysis. (**A**) Venn diagram of *SAGs* in different comparison groups. (**B**) The GO enrichment analysis of the 108 *SAGs* shared by all the comparison group. The X-axis indicates different GO terms. The left Y-axis represents the percentage of genes, and the right Y-axis represents the number of genes enriched for the relevant GO terms. (**C**) KEGG pathway enrichment analysis of the 108 *SAGs* shared by all the comparison group. The X-axis indicates enrichment factor, which represents the ratio of the proportion of genes annotated to a specific pathway among DEGs to the proportion of genes annotated to the same pathway among all genes. Dot color indicates *q*-value, which is the *p*-value corrected by multiple hypotheses testing.

| Number | Medicago truncatula Gene Id | Homologous Gene Id in Arabidopsis thaliana | Arabidopsis thaliana Gene Name | Effect for Senescence | Reference |
|--------|-----------------------------------|---|--------------------------------------|--------------------------|-----------|
| 1 | Medtr2g066830 | AT3G12830 | SAUR72 | Promote | [57] |
| 2 | Medtr1g100623 | AT5G52300 | RD29B | Delay | [30] |
| 3 | Medtr4g109830 | AT5G60910 | AGL8 | Promote | [58,59] |
| 4 | Medtr5g083270 | AT5G05440 | PYL5 | Promote | [60] |
| 5 | Medtr5g091390 | AT1G29860 | WRKY71 | Promote | [37] |
| 6 | Medtr8g018730 | AT1G55020 | LOX1 | Promote | [61] |
| 7 | Medtr8g074270 | AT3G51430 | YLS2 | Marker gene | [62] |

Table 1. Homologous genes involved in senescence regulation in Arabidopsis.

2.7. Transcription Factor Analysis

Transcription factors (TFs) are recognized as key regulators of leaf senescence. We employed Plant Transcription Factor Database (PlantTFDB v5.0) to perform TF prediction. Among the 108 *SAGs* analyzed, 7 TFs were annotated by PlantTFDB 5.0, which belong to bHLH (two genes), NF-X1, bZIP, MADS and WRKY (two genes) TF families (Figure 6A; Table S6). One of the identified WRKY TFs, homologs to WRKY71 in *Arabidopsis*, has been demonstrated to positively regulate leaf senescence. Nevertheless, there is currently no report about whether the remaining six genes also play a role in the regulation of leaf senescence, thus requiring further investigation.

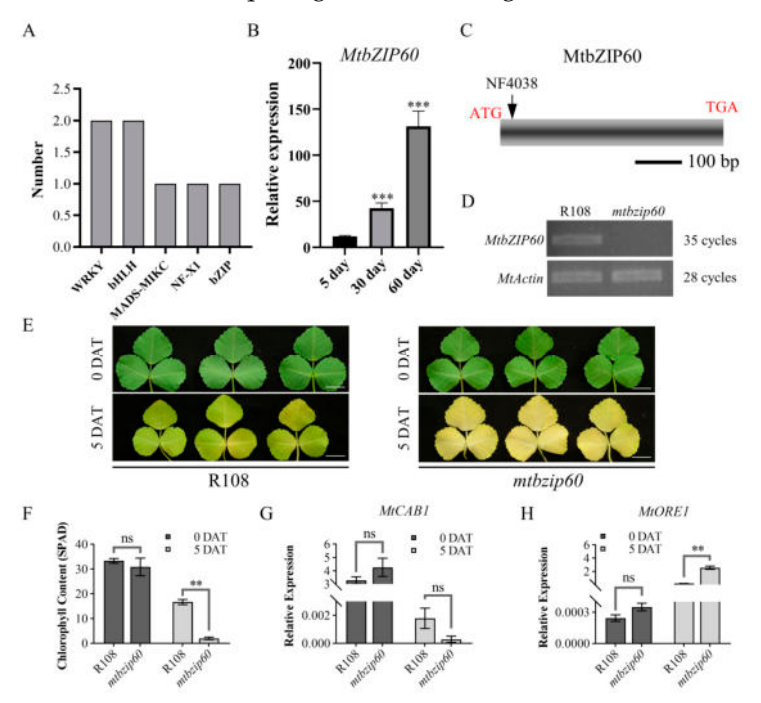


Figure 6. MtbZIP60 functions as negative regulator of leaf senescence. **(A)** Prediction of TFs within the 108 *SAGs*. **(B)** Expression trend of MtbZIP60 during leaf growth and senescence. **(C)** Schematic representation of the structure of MtbZIP60 and the position of Tnt1 in mtbzip60. **(D)** RT-PCR analysis of MtbZIP60 in wild type (R108) and mtbzip60. **(E)** Detached leaves of WT and mtbzip60 in the dark for 5 days. Bars = 1 cm. **(F)** Measurement of chlorophyll content (SPAD) in **(E)**. **(G,H)** qRT-PCR detection of MtCAB1 **(G)** and MtORE1 **(H)** transcriptional level in **(E)**. DAT, days after treatment. Date is shown as mean \pm SD. Asterisks indicate significant difference from the WT (Student's t test, ** p < 0.01, *** p < 0.001, ns: no significant). At least three biological replicates were performed.

2.8. MtbZIP60 Functions as a Novel Regulator of Leaf Senescence

As only a limited number of bZIP TFs have been identified as regulators of leaf senescence in different species, the identified bZIP TF MtbZIP60 was chosen to perform further functional analysis. We first validated the expression trend of MtbZIP60 during leaf

growth and senescence. The result showed a significant increase in *MtbZIP60* expression level as leaf aging (Figure 6B, Table S1). In order to investigate the roles of MtbZIP60, we obtained a *Tnt1*-inserted mutant line *mtbzip60* through screening the mutant collection. The *MtbZIP60* gene contains a single exon, with the *Tnt1* insertion at 16 bp downstream of the translational start codon (Figure 6C). qRT-PCR analysis showed that the insertion of *Tnt1* leads to the loss of full-length expression of *MtbZIP60* (Figure 6D). Dark treatment is an effective method to induce leaf senescence and is commonly used to simulate synchronous senescence [15]. Therefore, the fifth fully expanded compound leaf from apex was detached for dark treatment. After a five-day dark treatment, the detached leaves of *mtbzip60* showed an accelerated leaf senescence compared with the wild-type R108 (Figure 6E). The degradation of chlorophyll, as reflected by the SPAD value, was significant higher in *mtbzip60* compared with R108, which is consistent with the differences observed in the senescence process (Figure 6F). In addition, the senescence marker genes, *MtORE1* and *MtCAB1*, exhibited corresponding alterations as well (Figure 6G,H). These results suggested that MtbZIP60 acts as a novel regulator of leaf senescence in *M. truncatula*.

2.9. Expression Pattern, Subcellular Localization and Transcriptional Activity Analysis of MtbZIP60

qRT-PCR was performed to analyze the temporal and spatial expression of *MtbZIP60*. The result revealed that *MtbZIP60* exhibited relatively high-level expression in leaf, moderate-level expression in root and stem and low-level expression in pod and seed (Figure 7A). The observed peak expression in leaf is consistent with its regulatory role in leaf senescence.

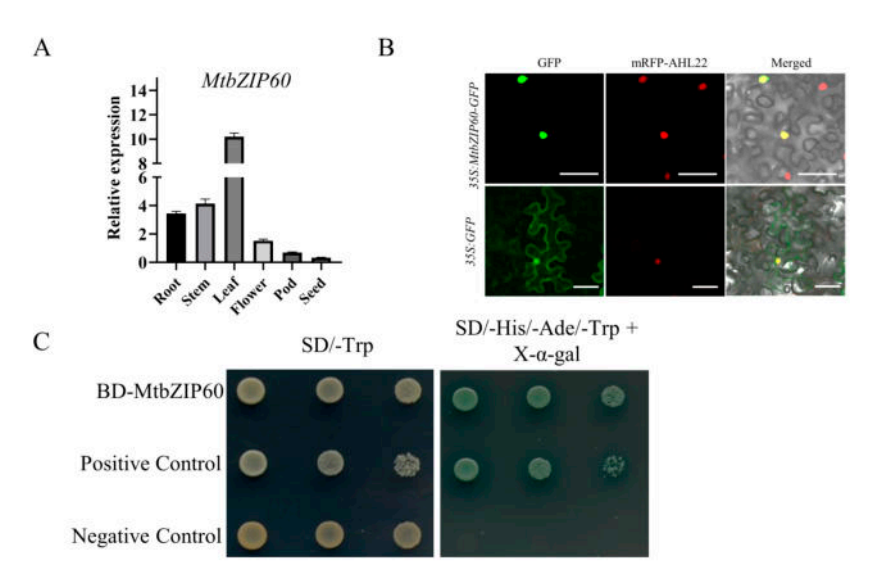


Figure 7. Expression pattern, subcellular localization and transcriptional activity analysis of MtbZIP60. (**A**) Expression pattern of MtbZIP60 in different tissues detected using qRT-PCR. MtActin was used as an internal control. (**B**) Subcellular localization of GFP and MtbZIP60-GFP in epidermal cells of tobacco leaf. The mRFP-AHL22 fusion was used as nuclear localization marker. Green represents the green fluorescent protein, red represents the red fluorescent protein, and yellow is obtained by combining the two fluorescent proteins. Bars = 20 μ m. (**C**) Transactivation activity analysis of MtbZIP60 in yeast. Full-length CDS of MtbZIP60 and TaNAC6 were cloned into the pGBKT7 vector and transformed into yeast strain AH109. Transformants harboring different plasmids were inoculated onto selective medium, with BD-TaNAC6 serving as the positive control.

To determine the subcellular localization of MtbZIP60, green fluorescent protein (GFP) was fused to the C-terminus of MtbZIP60 and expressed in tobacco epidermal cells, driven by the cauliflower mosaic virus 35S promoter. In contrast to the GFP control, where the fluorescence was detectable in both the cytoplasm and nucleus, the MtbZIP-GFP fluorescence specifically localized to the nucleus (Figure 7B).

To analyze the transcriptional activity of MtbZIP60, the CDS of MtbZIP60 was cloned into pGBKT7 vector, to generate GAL4BD-MtbZIP60 fusion. The pGBKT7 vector and GAL4BD-TaNAC6 were used as negative and positive controls, respectively [15]. Compared to the negative control, GAL4BD-MtbZIP60 and GAL4BD-TaNAC6 could activate the expression of reporter genes in yeast, as evidenced by normal growth on the selective SD medium lacking Trp, His and Ade (Figure 7C). The result indicates a potential involvement of MtbZIP60 in transcriptional regulation.

2.10. MtbZIP60 Interacts with MtWRKY40 in Regulation of Leaf Senescence

To elucidate the regulatory mechanism of MtbZIP60 in regulation leaf senescence, we conducted a yeast two-hybrid library screening to identify MtbZIP60-interacting proteins. The CDS of MtbZIP60 was cloned into pGBKT7, serving as a bait. The selective medium was supplemented with different concentrations of 3-AT to evaluate its inhibitory effect on the transactivation activity of MtbZIP60. The result showed that a concentration of 60 mM of 3-AT could completely inhibit the transcriptional activation activity of MtbZIP60 and be used for Y2H screening. A total of 72 clones were obtained and sequenced, out of which three copies were identified as a WRKY TF, MtWRKY40 (Medtr2g105060). We then amplified the CDS of MtWRKY40 and MtbZIP60 and constructed them into pGBKT7 vector and pGADT7 vector, respectively, for Y2H assay. The result showed that the yeast co-transformed with BD-MtWRKY40 and AD-MtbZIP60 could grow on SD/-Trp-His-Ade + X- α -gal medium, confirming the MtbZIP60-MtWRKY40 interaction in yeast (Figure 8A). The interaction was verified via a luciferase complementation imaging (LCI) assay in *Nicotiana benthamiana* using split luciferase protein. Strong luciferase (LUC) signal was detected in tobacco leaf between MtbZIP60-nLUC and cLUC-MtWRKY40, whereas no LUC signals were observed in the negative control (Figure 8B).

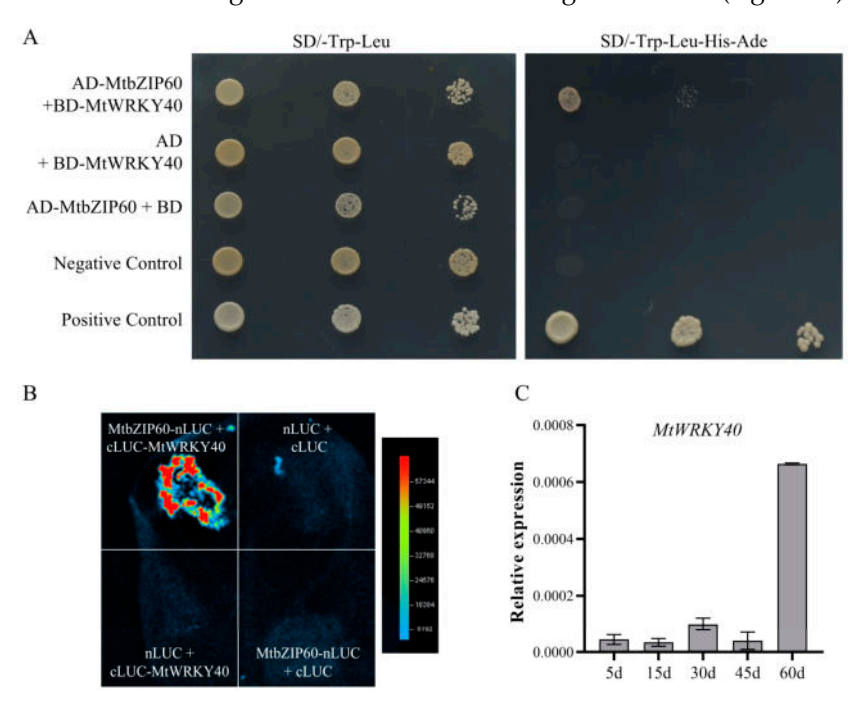


Figure 8. MtbZIP60 physically interacts with MtWRKY40 in the regulation of leaf senescence. (**A**) Interaction of MtbZIP60 and MtWRKY40 in an Y2H assay. Yeast cells were co-transformed with AD-MtbZIP60 and BD-MtWRKY40 and cultured on selective medium. Auxotrophic growth on the SD/-Trp-Leu-His-Ade medium indicates the interaction. (**B**) Interaction of MtbZIP60 and MtWRKY40 in *N.benthamiana* leaf using an LCI assay. MtbZIP60 was fused with the n-terminal of LUC to generate MtbZIP60-nLUC. MtWRKY40 was fused with the c-terminal of LUC to generate cLUC-MtWRKY40. Different pairs of constructs were used for infiltrating tobacco leaves. (**C**) Expression trend of *MtWRKY40* during leaf growth and senescence.

To determine the potential role of MtWRKY40 in leaf senescence, we analyzed its expression trend during leaf growth and senescence, and the result showed a significant

up-regulation in the 60-day-old senescent leaves, indicating MtWRKY40 may participate in the regulation of leaf senescence (Figure 8C). These results suggest MtbZIP60 inhibits leaf senescence through its interaction with MtWRKY40.

3. Discussion

Leaf senescence is a crucial issue in leaf development, closely related to the biomass production and quality of forage crops. Premature leaf senescence can lead to significant biomass loss and decreased nutritional quality, whereas delaying leaf senescence may serve as a feasible strategy to improve forage biomass production and quality. *M. truncatula* is a close relative of alfalfa. Investigating the regulatory mechanism behind leaf senescence in *M. truncatula* can provide valuable insights into how leaf senescence is controlled or could directly indicate the function of homologues genes in alfalfa. This is exemplified by the functional analysis of *SGR* in alfalfa, which is initially cloned from *M. truncatula*, with both performing a similar function in chlorophyll degradation [53]. Transcriptomic analyses are an efficient and reliable approach for identifying DEGs and have been utilized to screen for underling *SAGs* and TFs involved in regulating leaf senescence in various species, including wheat, rice, maize, foxtail millet, cotton, sorghum and *Arabidopsis*, which provide valuable insights into the mechanisms that govern this complicated biological process [63–67].

In this study, we examined age-dependent leaf senescence in *M. truncatula* and employed transcriptome analysis to investigate *SAGs*. To determine the optimal timing for sampling, we continuously monitored the growth and senescence process of leaves. During progression of senescence, malondialdehyde (MDA) and chlorophyll content are commonly utilized as indicators due to their noticeable alteration. Our data indicated that the chlorophyll content in leaves, as reflected by the SPAD value, peaked at 5 days after emergence and exhibited a significant downward trend from 30 to 60 days. Leaf yellowing became visible at 45 days and particularly prominent at 60 days, which corresponds to the chlorophyll content and the progression of leaf senescence (Figure 1A,B). The MDA content exhibited a decrease at 15 days and significant increase at 45 days and 60 days, consistent with the progression of leaf senescence. Our data suggested that the specific time points, 5 day, 30 day and 60 day, selected for transcriptomic analysis corresponded to the stages of the young leaf, mature leaf and senescent leaf, respectively.

As senescence advances, the expression of genes is closed linked to metabolic processes, including those related to the degradation of chlorophyl, amino acids, lipids, carbohydrates and nitrogen compounds [7,53,63]. In our study, we identified 108 genes that continuously up-regulated genes during leaf development and senescence, which appear to be involved in multiple regulatory pathways in leaf senescence. GO and KEGG enrichment analyses revealed that the identified *SAGs* were primarily enriched in nitrogen metabolism, amino acid metabolism, RNA degradation, linolenic acid metabolism and glutathione metabolism (Figure 4). These results provide insights into the physiological and biochemical changes that occur during leaf senescence in *M. truncatula*.

Activation of transcription factors (TFs) are one of the hallmarks during the initiation and progression of leaf senescence [13]. Over the past decades, considerable progress has been made in our comprehension of the TFs' functions in the regulation of leaf senescence [13,15,17]. Transcriptome analysis is also used for analysis and mining of TFs implicated in this process [7,56]. In our study, we predicted TFs within the obtained *SAGs* through the PlantTFDB database and found that TFs from the WRKY, bHLH, NF-X1 and bZIP families were identified, which play a role in senescence regulation (Figure 5A). Medtr5g091390, one of the predicted WRKY TFs, is homologous to WRKY71, which has been demonstrated to positively regulate leaf senescence via multiple pathways in *Arabidopsis thaliana* [37]. Thus, there are reasons to believe that Medtr5g091390 may also participate in the regulation of leaf senescence, even though its function is currently ambiguous and warrants further investigation. Other TFs, MTR_2g038040 (bHLH), MTR_4g027040 (NF-X1), MTR_4g131160 (bHLH) and MTR_4g122530 (WRKY), were continuously up-regulated

during leaf senescence yet have not been proved to be directly involved in the regulation of leaf senescence and deserve further investigation.

WRKY and NAC are the most extensively studied TF families that regulate leaf senescence [13,14]. Additionally, the bZIP family is also essential in this biological process, although fewer members have been cloned [41]. Through transcriptome analysis, a novel bZIP TF MtbZIP60 was identified as exhibiting a continuously up-regulated expression pattern throughout leaf growth and senescence. Phenotypic analysis of the Tnt1 retrotransposon-tagged mutant line *mtbzip60*, which lacks the full-length transcript, demonstrated a delayed leaf senescence phenotype, suggesting that MtbZIP60 acts as a negative regulator of leaf senescence (Figure 5). Additional phenotypic evaluation of MtbZIP60 overexpression in suppressing leaf senescence will provide more solid evidence to validate its negative impact on leaf senescence regulation. Subcellular localization analysis revealed MtbZIP60 is localized in the nucleus and exhibits transcriptional activation activity, suggesting its protentional involvement in transcriptional regulation (Figure 7). We also found that MtbZIP60 can associate with MtWRKY40, which also showed an up-regulated pattern during leaf senescence (Figure 7), whereas the precise role of MtWRKY40 in leaf senescence regulation requires additional investigation. Further research on MtbZIP60 and its interaction with MtWRKY40 in the regulation of leaf senescence in M. truncatula will enhance our understanding of the transcriptional regulation mechanism underlying leaf senescence.

Leaf senescence is pivotal for plant growth, stress tolerance, reproductivity and fitness. In crops, the timing of leaf senescence profoundly influences grain yield and nutritional quality, making it a key agronomic trait [68]. In forage crops where nutrients are primarily stored in leaves, leaf senescence may directly affect the overall forage quality [8]. Alfalfa is one of the most important legume forage species in the world due to its high yield, nutritional quality and adaptability. It is believed that preventing premature leaf senescence and cultivation of new varieties of alfalfa with optimized leaf senescence are effective ways to improve the quantity and quality of alfalfa [7,8,51]. In our study, we conducted a systematical analysis of the dynamic gene expression pattern during leaf senescence in M. truncatula, a close relative of alfalfa, and obtained a series of SAGs in which MtbZIP60 was identified as a positive regulator. Identification of homologous genes to MtbZIP60 in alfalfa and investigation of its precise function in regulating leaf senescence are essential. Further evaluating its practical influence on forage yield and quality under field conditions could not only help our comprehension of the mechanism involved in this process in alfalfa, but it may also provide valuable gene resources and practical methods for cultivating new alfalfa varieties with manipulated leaf senescence processes.

4. Material and Methods

4.1. Plant Materials and Growth Condition

The *M. truncatula* ecotype R108 was used in this study. NF4038 (*mtbzip60*) was obtained by screening tobacco retrotransposon *Tnt1*-tagged mutant collection of *M. truncatula*. For germination, seeds were sown to petri dishes with moistened filter paper after imbibition, followed by a 7-day stratification at 4 °C. Subsequently, the dishes were then moved to a growth chamber overnight to promote seed germination at 24 °C. The germinated seeds were then grown in the greenhouse under the following conditions: 24 °C day/20 °C night temperature, 16-h day/8-h night photoperiod and 60% to 70% relative humidity. The fifth compound leaves were harvested at 5 d, 30 d and 60 d after emerging and frozen in liquid nitrogen. Three biological repeats were prepared, each comprising individual leaf from five plants.

4.2. Determination of Chlorophylls and MDA Content

The determination of chlorophyll content was carried out using a SPAD 502 Plus Chlorophyll Meter (Konica Minolta, Tokyo, Japan), with reads indicated as SPAD values.

The measurement of malondialdehyde (MDA) content was performed through thiobarbituric acid (TBA) reaction, as described by Saher [69]. Briefly, 0.5 g of leaf tissue was

homogenized by grinding in liquid nitrogen, followed by adding $10 \, \mathrm{mL} \ 0.1\%$ trichloroacetic acid (TCA) and vortex mixing. The homogenate was then centrifuged at $12,000 \, \mathrm{rpm}$ for $5 \, \mathrm{min}$ and $4 \, \mathrm{mL} \ 20\%$ TCA containing 0.5% TBA were add to $1 \, \mathrm{mL}$ of the supernatant. The mixture was heated and rapidly cooled down in an ice slurry. After centrifugation, the absorbance of the solution was measured at wavelengths of $450 \, \mathrm{nm}$, $532 \, \mathrm{nm}$ and $600 \, \mathrm{nm}$. The concentration of MDA was calculated using an extinction coefficient of $155 \, \mathrm{mM}^{-1} \, \mathrm{cm}^{-1}$.

4.3. RNA Isolation and Gene Expression Analysis

Total RNA was extracted Using TRIzol® Reagent (TAKARA, Cat#9109, Kusatsu, Shiga, Japan). First strand cDNA was synthesized from 1 µg of total RNA using HiScript® II QRT Super-Mix (Vazyme, R222-01, Nanjing, China) according to the manufacturer's instructions. RT-PCR was performed at 98 °C for 5 min, followed by 28–40 cycles of amplification (98 °C for 20 s, 55–60 °C for 20 s and 72 °C for 20 s). Quantitative RT-PCR was performed on a CFX96 Real-Time System (Bio-Rad, Hercules, CA, USA) with ChamQ SYBR qPCR Master Mix (Vazyme, Q711-02). The qRT-PCR reaction consists of 10.0 µL of 2 × ChamQ Universal SYBR qPCR Master Mix, along with 0.4 µL each of forward and reverse primers, and template cDNA, reaching a total volume of 20 µL. Relative gene expression levels were calculated using the $2^{-\Delta\Delta Ct}$ method with a *M. truncatula ACTIN* gene as internal control. The qRT-PCR were performed with at least three biological replicates, each containing four technical replicates. qRT-PCR primers were designed using Primer3web version 4.1.0. All primers used in this study are listed in Supplementary Table S1.

4.4. Library Construction and Transcriptome Sequencing

Total RNA was extracted from leaves at different developmental stages. RNA concentration and purity was analyzed using NanoDrop 2000 (Thermo Fisher Scientific, Wilmington, DE, USA). RNA integrity was assessed using the RNA Nano 6000 Assay Kit of the Agilent Bioanalyzer 2100 system (Agilent Technologies, Santa Clara, CA, USA). RNA libraries were generated using the NEBNext® UltraTM RNA Library Prep Kit for Illumina® (NEB, Ipswich, MA, USA) based on manufacturer's guidelines. In brief, mRNA was purified using oligo (dT) beads and fragmented with fragmentation buffer. Double-stranded cDNA was obtained using a double-stranded cDNA synthesis kit (NEB, Ipswich, MA, USA). After an "A" base was added to the 3' ends of DNA fragments, NEBNext Adaptor with hairpin loop structure were ligated. Then, the library fragments were purified with AMPure XP system (Beckman Coulter, Beverly, CA, USA) to select for ~240 bp cDNA fragments, followed by PCR amplified using Phusion High-Fidelity DNA polymerase (NEB, Ipswich, MA, USA). After purification of PCR products, library quality was assessed on the Agilent Bioanalyzer 2100 system. Clustering was performed on a cBot Cluster Generation System using TruSeq PE Cluster Kit v4-cBot-HS (Illumia), and RNA-seq sequencing library was carried out on Illumina NovaSeq 6000 platform.

The raw reads were processing through in-house Perl scripts, and obtained clean reads were mapped to M. truncatula reference genome (http://plants.ensembl.org/Medicago_truncatula/Info/Index (accessed on 1 March 2022) using Hisat2 2.0.4 (http://ccb.jhu.edu/software/hisat2/index.shtml (accessed on 20 March 2022)). The gene expression level was indicated as cDNA fragments per kilobase per million fragments that mapped to the M. truncatula reference genome. Differentially expressed genes (DEGs) between different samples were obtained using DESeq2 1.6.3 with adjusted p-value < 0.01 and $|\log_2|$ (fold change) |>1 or <-1.

4.5. Transcription Factor Analysis

The Plant Transcription Factor Database (PlantTFDB 5.0, https://planttfdb.gao-lab.org/prediction.php (accessed on 5 May 2022)) was used with the default parameters to perform TF prediction according to the domain information contained.

4.6. Gene Ontology and Kyto Encyclopedia of Genes and Genomes Pathway Enrichment Analysis

The Gene Ontology (GO) and Kyto Encyclopedia of Genes and Genomes (KEGG) pathway enrichment analyses were performed on the platform BMKCloud (www.biocloud.net (accessed on 25 March 2022)). Specifically, GO enrichment analysis was implemented by the GOseq R packages (3.19)-based Wallenius non-central hyper-geometric distribution (accessed on 5 April 2022) [70], which can adjust for gene length bias in DEGs. KOBAS 2.0 [71] software (accessed on 10 April 2022) was used to test the statistical enrichment of differential expression genes in KEGG pathways.

4.7. Protein Subcellular Localization

The coding sequence of MtbZIP60 was amplified and introduced into Gateway binary vector pMDC83. Construct of GFP was used as positive control and mRFP-AHL22 as nuclear localized marker. The obtained vector was transformed into Agrobacterium tumefaciens strain GV2260 and then used to infiltrate tobacco leaves in the infiltration buffer, consisting of 10 mM 2-morpholinoethanesulphonic acid (MES, pH = 5.8), 200 μ M acetosyringone and 10 mM MgCl₂. The final OD₆₀₀ of each recombinant Agrobacterium tumefaciens strain was 0.5. Abaxial sides of the 4th and 5th leaves of 4-week-old tobacco (N. benthamiana) leaves from the top were selected and infiltrated with the Agrobacterium tumefaciens mixture. The infiltrated tobaccos were grown in the dark for 12 h before being transferred to the greenhouse, where they were sampled after 3 days for investigation. GFP-MtbZIP60 signal was examined using Olympus FV3000 confocal microscopy.

4.8. Transactivation Activity Assay in Yeast

The coding sequence of MtbZIP60 was cloned into pGBKT7 to generate GAL4BD-MtbZIP60 fusion. The resulting constructs and positive control GAL4BD-TaNAC6 were transformed into Saccharomyces cerevisiae strain AH109, respectively. The transformed yeast was then screened on SD/-Trp medium. Positive recombinant clones were resuspended with sterilized water and inoculated on SD/-Trp-His-Ade + X- α -gal for analysis of transactivation activity.

4.9. Yeast Two-Hybrid (Y2H) Interactions and Library Screening

The Y2H cDNA library was constructed by OE biotech (Shanghai, China) via cloning the full-length cDNA library prepared from different tissues into the pGADT7 vector and transformed into yeast Y187 strain. The coding sequence of MtbZIP60 was inserted into the pGBKT7 vector, fusing with GAL4BD. The resulting construct was transformed into yeast strain AH109 and mated with the cDNA library. After mating, cultures were spread on 35 large Petri dishes containing SD/-Ade-His-Leu-Trp supplied with 60 mM of 3-AT to inhibit the transactivation activity of MtbZIP60 and 20 μ g/mL X- α -gal for blue colony selection and incubated for 3–5 days at 28 °C. The coding sequences of identified candidates were amplified, sequenced and cloned for further validation.

For pairwise Y2H assay, it was performed as previous described [72]. The full-length CDSs of candidates were amplified and inserted into the *pGADT7* vector. Then, the prey and bait plasmids were co-transformed into yeast strain AH109 and incubated on SD/-Leu-Trp and SD/-Ade-His-Leu-Trp selective media to test for interaction.

4.10. Luciferase Complementation Imaging Assay (LCI)

The LCI assay was performed as previous described [73]. The CDSs of MtbZIP60 and MtWRKY40 were amplified and used to subclone the different constructs (MtbZIP60-nLuc, cLuc-MtWRKY40). Agrobacterium cells (GV3101) containing different pair of plasmids were adjusted to optical density (OD_{0.5-0.6}) with infiltration buffer and infiltrated into tobacco leaves. After incubation in the dark for 12 h and normal culture for 3 days, the luciferase substrates (D-luciferin potassium salt, LUCK, GOLDBIO) were sprayed onto the infiltrated leaves and further analyzed by a low-light cooled charge-coupled imaging device (VILBER, FUSION FX7 Spectra).

4.11. Statistical Analysis

Unless particularly stated, statistical significance test was conducted by a two-tailed Student's t-test. Differences were considered statistically significant when $p \le 0.05$. * and ** indicate p < 0.05 and p < 0.01, respectively.

4.12. Accession Number

The gene sequence can be accessed via Phytozome (https://phytozome-next.jgi.doe.gov/ (accessed on 7 September 2022)) database under the following accession numbers: *MtbZIP60* (Medtr4g070860), *MtWRKY40* (Medtr2g105060), *MtORE1* (Medtr4g108760), *Mt-CAB1* (Medtr4g094605), which are based on ecotype A17 genome sequence.

5. Conclusions

In summary, we carried out a comparative transcriptome analysis using young, mature and senescent leaves of *M. truncatula*. A total of 1057 DEGs were obtained, in which 108 genes exhibited a consistently up-regulated pattern during leaf senescence. Seven TFs were identified within the 108 *SAGs*, and a novel bZIP TF MtbZIP60 was demonstrated to negatively regulate leaf senescence through interacting with MtWRKY40. Our results help shed light on the transcriptional regulation mechanisms underlying leaf senescence in *M. truncatula* and provide potential targets for manipulating leaf senescence progression to improve the biomass yield and quality of alfalfa.

Supplementary Materials: The following supporting information can be downloaded at: https://www.mdpi.com/article/10.3390/ijms251910410/s1.

Author Contributions: Conceptualization, P.Y., C.Z. and G.W.; validation, J.X., J.W. (Jialan Wang) and J.C.; formal analysis, K.L. and X.M.; Resources, J.W. (Jiangqi Wen) and K.S.M.; writing—original draft preparation, P.Y. All authors have read and agreed to the published version of the manuscript.

Funding: This research was funded by grants from the Hebei Natural Science Foundation(C2022205015, C2022205038 and C2023205050), the Modern Agro-industry Technology Research Team of Hebei (HBCT2024030201) and the Postdoctoral Preferred Funding Research Project of Hebei Province (B2021003018).

Data Availability Statement: The datasets present in this study can be found within the article and its supplemental data. The transcriptome raw data can be found at the NCBI database with the project ID1131009 (http://www.ncbi.nlm.nih.gov/bioproject/1131009 (accessed on 23 September 2024)).

Conflicts of Interest: The authors declare no conflicts of interest.

References

- 1. Guo, Y.; Ren, G.; Zhang, K.; Li, Z.; Miao, Y.; Guo, H. Leaf senescence: Progression, regulation, and application. *Mol. Hortic.* **2021**, 1, 5. [CrossRef] [PubMed]
- 2. Woo, H.R.; Kim, H.J.; Lim, P.O.; Nam, H.G. Leaf senescence: Systems and dynamics aspects. *Annu. Rev. Plant Biol.* **2019**, 70, 347–376. [CrossRef] [PubMed]
- 3. Gregersen, P.L.; Holm, P.B.; Krupinska, K. Leaf senescence and nutrient remobilisation in barley and wheat. *Plant Biol.* **2008**, *10* (Suppl. S1), 37–49. [CrossRef]
- 4. Gregersen, P.L.; Culetic, A.; Boschian, L.; Krupinska, K. Plant senescence and crop productivity. *Plant Mol. Biol.* **2013**, *82*, 603–622. [CrossRef]
- 5. Kim, T.; Kang, K.; Kim, S.H.; An, G.; Paek, N.C. *OsWRKY5* promotes rice leaf senescence via senescence-associated NAC and abscisic acid biosynthesis pathway. *Int. J. Mol. Sci.* **2019**, 20, 4437. [CrossRef]
- 6. Joshi, S.; Choukimath, A.; Isenegger, D.; Panozzo, J.; Spangenberg, G.; Kant, S. Improved wheat growth and yield by delayed leaf senescence using developmentally regulated expression of a cytokinin biosynthesis gene. *Front. Plant Sci.* **2019**, *10*, 1285. [CrossRef]
- 7. Dong, S.; Sang, L.; Xie, H.; Chai, M.; Wang, Z.Y. Comparative Transcriptome analysis of salt stress-induced leaf senescence in *Medicago truncatula*. Front. Plant Sci. **2021**, 12, 666660. [CrossRef] [PubMed]
- 8. Zhang, K.; Xie, H.; Wen, J.; Zhang, J.; Wang, Z.-Y.; Xu, B.; Chai, M. Leaf Senescence in Forage and Turf Grass: Progress and Prospects; Maximum Academic Press: Fayetteville, GA, USA, 2024; Volume 4. [CrossRef]
- 9. Li, Z.; Oelmüller, R.; Guo, H.; Miao, Y. Editorial: Signal transduction of plant organ senescence and cell death. *Front. Plant Sci.* **2023**, *14*, 1172373. [CrossRef]

10. Ostrowska-Mazurek, A.; Kasprzak, P.; Kubala, S.; Zaborowska, M.; Sobieszczuk-Nowicka, E. Epigenetic landmarks of leaf senescence and crop improvement. *Int. J. Mol. Sci.* **2020**, *21*, 5125. [CrossRef]

- 11. Guo, Y.; Gan, S. Leaf senescence: Signals, execution, and regulation. Curr. Top. Dev. Biol. 2005, 71, 83-112. [CrossRef]
- 12. Lim, P.O.; Kim, H.J.; Nam, H.G. Leaf senescence. Annu. Rev. Plant Biol. 2007, 58, 115–136. [CrossRef] [PubMed]
- 13. Cao, J.; Liu, H.; Tan, S.; Li, Z. Transcription factors-regulated leaf senescence: Current knowledge, challenges and approaches. *Int. J. Mol. Sci.* 2023, 24, 9245. [CrossRef] [PubMed]
- 14. Bengoa Luoni, S.; Astigueta, F.H.; Nicosia, S.; Moschen, S.; Fernandez, P.; Heinz, R. Transcription factors associated with leaf senescence in crops. *Plants* **2019**, *8*, 411. [CrossRef]
- 15. Li, J.; Qiao, H.; Yin, P.; Liu, M.; Yang, Y.; Li, K.; Yang, L.; Yang, C.; Zhao, L.; Zhou, S.; et al. Increasingly amplified stimulation mediated by TaNAC69-B is crucial for the leaf senescence in wheat. *Plant J.* **2023**, *114*, 570–590. [CrossRef]
- 16. Miao, Y.; Laun, T.; Zimmermann, P.; Zentgraf, U. Targets of the WRKY53 transcription factor and its role during leaf senescence in *Arabidopsis. Plant Mol. Biol.* **2004**, 55, 853–867. [CrossRef]
- 17. Lu, M.; Fu, B.; Meng, X.; Jia, T.; Lu, X.; Yang, C.; Li, K.; Yin, P.; Guo, Y.; Li, W.; et al. *NtNAC028* and *NtNAC080* form heterodimers to regulate jasmonic acid biosynthesis during leaf senescence in *Nicotiana tabacum*. *J. Exp. Bot.* **2024**, 75, 2351–2371. [CrossRef]
- 18. Chen, Q.; Yan, J.; Tong, T.; Zhao, P.; Wang, S.; Zhou, N.; Cui, X.; Dai, M.; Jiang, Y.Q.; Yang, B. ANAC087 transcription factor positively regulates age-dependent leaf senescence through modulating the expression of multiple target genes in *Arabidopsis*. *J. Integr. Plant Biol.* 2023, 65, 967–984. [CrossRef] [PubMed]
- 19. Garapati, P.; Xue, G.P.; Munné-Bosch, S.; Balazadeh, S. Transcription factor *ATAF1* in *Arabidopsis* promotes senescence by direct regulation of key chloroplast maintenance and senescence transcriptional cascades. *Plant Physiol.* **2015**, *168*, 1122–1139. [CrossRef]
- 20. Kim, Y.S.; Sakuraba, Y.; Han, S.H.; Yoo, S.C.; Paek, N.C. Mutation of the *Arabidopsis NAC016* transcription factor delays leaf senescence. *Plant Cell Physiol.* **2013**, *54*, 1660–1672. [CrossRef]
- 21. Takasaki, H.; Maruyama, K.; Takahashi, F.; Fujita, M.; Yoshida, T.; Nakashima, K.; Myouga, F.; Toyooka, K.; Yamaguchi-Shinozaki, K.; Shinozaki, K. SNAC-As, stress-responsive NAC transcription factors, mediate ABA-inducible leaf senescence. *Plant J.* 2015, 84, 1114–1123. [CrossRef]
- 22. Guo, Y.; Gan, S. AtNAP, a NAC family transcription factor, has an important role in leaf senescence. *Plant J.* **2006**, *46*, 601–612. [CrossRef] [PubMed]
- 23. Mahmood, K.; El-Kereamy, A.; Kim, S.H.; Nambara, E.; Rothstein, S.J. *ANAC032* positively regulates age-dependent and stress-induced senescence in *Arabidopsis thaliana*. *Plant Cell Physiol*. **2016**, 57, 2029–2046. [CrossRef] [PubMed]
- 24. Oda-Yamamizo, C.; Mitsuda, N.; Sakamoto, S.; Ogawa, D.; Ohme-Takagi, M.; Ohmiya, A. The NAC transcription factor *ANAC046* is a positive regulator of chlorophyll degradation and senescence in *Arabidopsis* leaves. *Sci. Rep.* **2016**, *6*, 23609. [CrossRef]
- 25. Balazadeh, S.; Kwasniewski, M.; Caldana, C.; Mehrnia, M.; Zanor, M.I.; Xue, G.P.; Mueller-Roeber, B. ORS1, an H₂O₂-responsive NAC transcription factor, controls senescence in *Arabidopsis thaliana*. *Mol. Plant* **2011**, *4*, 346–360. [CrossRef] [PubMed]
- 26. Li, S.; Gao, J.; Yao, L.; Ren, G.; Zhu, X.; Gao, S.; Qiu, K.; Zhou, X.; Kuai, B. The role of *ANAC072* in the regulation of chlorophyll degradation during age- and dark-induced leaf senescence. *Plant Cell Rep.* **2016**, *35*, 1729–1741. [CrossRef]
- 27. Balazadeh, S.; Siddiqui, H.; Allu, A.D.; Matallana-Ramirez, L.P.; Caldana, C.; Mehrnia, M.; Zanor, M.I.; Kohler, B.; Mueller-Roeber, B. A gene regulatory network controlled by the NAC transcription factor ANAC092/AtNAC2/ORE1 during salt-promoted senescence. *Plant J.* 2010, 62, 250–264. [CrossRef]
- 28. Kim, H.J.; Park, J.H.; Kim, J.; Kim, J.J.; Hong, S.; Kim, J.; Kim, J.H.; Woo, H.R.; Hyeon, C.; Lim, P.O.; et al. Time-evolving genetic networks reveal a NAC troika that negatively regulates leaf senescence in *Arabidopsis*. *Proc. Natl. Acad. Sci. USA* **2018**, 115, E4930–E4939. [CrossRef]
- 29. Wu, A.; Allu, A.D.; Garapati, P.; Siddiqui, H.; Dortay, H.; Zanor, M.I.; Asensi-Fabado, M.A.; Munné-Bosch, S.; Antonio, C.; Tohge, T.; et al. JUNGBRUNNEN1, a reactive oxygen species-responsive NAC transcription factor, regulates longevity in *Arabidopsis*. *Plant Cell* **2012**, 24, 482–506. [CrossRef]
- 30. Yang, S.D.; Seo, P.J.; Yoon, H.K.; Park, C.M. The *Arabidopsis* NAC transcription factor *VNI2* integrates abscisic acid signals into leaf senescence via the COR/RD genes. *Plant Cell* **2011**, 23, 2155–2168. [CrossRef]
- 31. Kan, C.; Zhang, Y.; Wang, H.L.; Shen, Y.; Xia, X.; Guo, H.; Li, Z. Transcription factor *NAC075* delays leaf senescence by deterring reactive oxygen species accumulation in *Arabidopsis*. *Front. Plant Sci.* **2021**, *12*, 634040. [CrossRef]
- 32. Jiang, J.; Ma, S.; Ye, N.; Jiang, M.; Cao, J.; Zhang, J. WRKY transcription factors in plant responses to stresses. *J. Integr. Plant Biol.* **2017**, *59*, 86–101. [CrossRef] [PubMed]
- 33. Robatzek, S.; Somssich, I.E. Targets of *AtWRKY6* regulation during plant senescence and pathogen defense. *Genes Dev.* **2002**, 16, 1139–1149. [CrossRef]
- 34. Zhou, X.; Jiang, Y.; Yu, D. *WRKY22* transcription factor mediates dark-induced leaf senescence in *Arabidopsis*. *Mol. Cells* **2011**, 31, 303–313. [CrossRef]
- 35. Niu, F.; Cui, X.; Zhao, P.; Sun, M.; Yang, B.; Deyholos, M.K.; Li, Y.; Zhao, X.; Jiang, Y.Q. WRKY42 transcription factor positively regulates leaf senescence through modulating SA and ROS synthesis in *Arabidopsis thaliana*. *Plant J.* **2020**, 104, 171–184. [CrossRef]
- 36. Zhang, H.; Zhang, L.; Wu, S.; Chen, Y.; Yu, D.; Chen, L. *AtWRKY75* positively regulates age-triggered leaf senescence through gibberellin pathway. *Plant Divers.* **2021**, *43*, 331–340. [CrossRef]
- 37. Yu, Y.; Qi, Y.; Xu, J.; Dai, X.; Chen, J.; Dong, C.H.; Xiang, F. *Arabidopsis WRKY71* regulates ethylene-mediated leaf senescence by directly activating EIN2, ORE1 and ACS2 genes. *Plant J.* **2021**, *107*, 1819–1836. [CrossRef]

38. Chen, L.; Xiang, S.; Chen, Y.; Li, D.; Yu, D. *Arabidopsis WRKY45* Interacts with the DELLA protein RGL1 to positively regulate age-triggered leaf senescence. *Mol. Plant* **2017**, *10*, 1174–1189. [CrossRef] [PubMed]

- 39. Besseau, S.; Li, J.; Palva, E.T. *WRKY54* and *WRKY70* co-operate as negative regulators of leaf senescence in *Arabidopsis thaliana*. *J. Exp. Bot.* **2012**, *63*, 2667–2679. [CrossRef] [PubMed]
- 40. Wang, Y.; Cui, X.; Yang, B.; Xu, S.; Wei, X.; Zhao, P.; Niu, F.; Sun, M.; Wang, C.; Cheng, H.; et al. *WRKY55* transcription factor positively regulates leaf senescence and the defense response by modulating the transcription of genes implicated in the biosynthesis of reactive oxygen species and salicylic acid in *Arabidopsis*. *Development* **2020**, 147, dev189647. [CrossRef]
- 41. Smykowski, A.; Fischer, S.M.; Zentgraf, U. Phosphorylation affects dna-binding of the senescence-regulating bZIP transcription factor GBF1. *Plants* **2015**, *4*, 691–709. [CrossRef]
- 42. Gao, S.; Gao, J.; Zhu, X.; Song, Y.; Li, Z.; Ren, G.; Zhou, X.; Kuai, B. ABF2, ABF3, and ABF4 promote ABA-mediated chlorophyll degradation and leaf senescence by transcriptional activation of chlorophyll catabolic genes and *senescence-associated genes* in *Arabidopsis*. *Mol. Plant* **2016**, *9*, 1272–1285. [CrossRef] [PubMed]
- 43. Zhao, G.; Cheng, Q.; Zhao, Y.; Wu, F.; Mu, B.; Gao, J.; Yang, L.; Yan, J.; Zhang, H.; Cui, X.; et al. The abscisic acid-responsive element binding factors MAPKKK18 module regulates abscisic acid-induced leaf senescence in *Arabidopsis*. *J. Biol. Chem.* 2023, 299, 103060. [CrossRef] [PubMed]
- 44. Hickman, R.; Hill, C.; Penfold, C.A.; Breeze, E.; Bowden, L.; Moore, J.D.; Zhang, P.; Jackson, A.; Cooke, E.; Bewicke-Copley, F.; et al. A local regulatory network around three NAC transcription factors in stress responses and senescence in *Arabidopsis* leaves. *Plant J.* **2013**, 75, 26–39. [CrossRef] [PubMed]
- 45. Li, X.; Li, X.; Li, M.; Yan, Y.; Liu, X.; Li, L. Dual function of NAC072 in ABF3-mediated ABA-responsive gene regulation in *Arabidopsis. Front. Plant Sci.* **2016**, 7, 1075. [CrossRef] [PubMed]
- 46. Zhang, Z.; Liu, C.; Li, K.; Li, X.; Xu, M.; Guo, Y. CLE14 functions as a "brake signal" to suppress age-dependent and stress-induced leaf senescence by promoting JUB1-mediated ROS scavenging in *Arabidopsis*. *Mol. Plant* **2022**, *15*, 179–188. [CrossRef]
- 47. Chen, D.; Shi, Y.; Zhang, P.; Xie, W.; Li, S.; Xiao, J.; Yuan, M. Deletion of the sugar importer gene *OsSWEET1b* accelerates sugar starvation-promoted leaf senescence in rice. *Plant Physiol.* **2024**, *195*, 2176–2194. [CrossRef] [PubMed]
- 48. Cui, J.; Wang, X.; Wei, Z.; Jin, B. Medicago truncatula (model legume), Medicago sativa (alfalfa), Medicago polymorpha (bur clover), and Medicago ruthenica. Trends Genet. 2022, 38, 782–783. [CrossRef]
- 49. Chen, H.; Zeng, Y.; Yang, Y.; Huang, L.; Tang, B.; Zhang, H.; Hao, F.; Liu, W.; Li, Y.; Liu, Y.; et al. Allele-aware chromosome-level genome assembly and efficient transgene-free genome editing for the autotetraploid cultivated alfalfa. *Nat. Commun.* 2020, 11, 2494. [CrossRef]
- 50. Shen, C.; Du, H.; Chen, Z.; Lu, H.; Zhu, F.; Chen, H.; Meng, X.; Liu, Q.; Liu, P.; Zheng, L.; et al. The chromosome-level genome sequence of the autotetraploid alfalfa and resequencing of core germplasms provide genomic resources for alfalfa research. *Mol. Plant* 2020, *13*, 1250–1261. [CrossRef]
- 51. Calderini, O.; Bovone, T.; Scotti, C.; Pupilli, F.; Piano, E.; Arcioni, S. Delay of leaf senescence in *Medicago sativa* transformed with the ipt gene controlled by the senescence-specific promoter SAG12. *Plant Cell Rep.* **2007**, *26*, 611–615. [CrossRef]
- 52. Jiang, J.; Jia, H.; Feng, G.; Wang, Z.; Li, J.; Gao, H.; Wang, X. Overexpression of Medicago sativa TMT elevates the α-tocopherol content in *Arabidopsis* seeds, alfalfa leaves, and delays dark-induced leaf senescence. *Plant Sci.* **2016**, 249, 93–104. [CrossRef] [PubMed]
- 53. Zhou, C.; Han, L.; Pislariu, C.; Nakashima, J.; Fu, C.; Jiang, Q.; Quan, L.; Blancaflor, E.B.; Tang, Y.; Bouton, J.H.; et al. From model to crop: Functional analysis of a STAY-GREEN gene in the model legume *Medicago truncatula* and effective use of the gene for alfalfa improvement. *Plant Physiol.* **2011**, *157*, 1483–1496. [CrossRef] [PubMed]
- 54. Li, S.; Xie, H.; Zhou, L.; Dong, D.; Liu, Y.; Jia, C.; Han, L.; Chao, Y.; Chen, Y. Overexpression of MsSAG113 gene promotes leaf senescence in alfalfa via participating in the hormone regulatory network. *Front. Plant Sci.* **2022**, *13*, 1085497. [CrossRef]
- 55. Mahmood, K.; Torres-Jerez, I.; Krom, N.; Liu, W.; Udvardi, M.K. Transcriptional programs and regulators underlying age-dependent and dark-induced senescence in *Medicago truncatula*. *Cells* **2022**, *11*, 1570. [CrossRef]
- 56. Dong, S.; Pang, W.; Liu, Z.; Li, H.; Zhang, K.; Cong, L.; Yang, G.; Wang, Z.Y.; Xie, H. Transcriptome analysis of leaf senescence regulation under alkaline stress in *Medicago truncatula*. Front. Plant Sci. **2022**, 13, 881456. [CrossRef]
- 57. Wen, Z.; Mei, Y.; Zhou, J.; Cui, Y.; Wang, D.; Wang, N.N. SAUR49 can positively regulate leaf senescence by suppressing SSPP in *Arabidopsis*. *Plant Cell Physiol*. **2020**, *61*, 644–658. [CrossRef] [PubMed]
- 58. Melzer, S.; Lens, F.; Gennen, J.; Vanneste, S.; Rohde, A.; Beeckman, T. Flowering-time genes modulate meristem determinacy and growth form in *Arabidopsis thaliana*. *Nat. Genet.* **2008**, *40*, 1489–1492. [CrossRef]
- 59. Breeze, E.; Harrison, E.; McHattie, S.; Hughes, L.; Hickman, R.; Hill, C.; Kiddle, S.; Kim, Y.S.; Penfold, C.A.; Jenkins, D.; et al. High-resolution temporal profiling of transcripts during *Arabidopsis* leaf senescence reveals a distinct chronology of processes and regulation. *Plant Cell* **2011**, 23, 873–894. [CrossRef]
- 60. Zhao, Y.; Zhang, Z.; Gao, J.; Wang, P.; Hu, T.; Wang, Z.; Hou, Y.J.; Wan, Y.; Liu, W.; Xie, S.; et al. *Arabidopsis* duodecuple mutant of PYL ABA receptors reveals PYL repression of ABA-independent SnRK2 activity. *Cell Rep.* **2018**, *23*, 3340–3351.e5. [CrossRef]
- 61. He, Y.; Fukushige, H.; Hildebrand, D.F.; Gan, S. Evidence supporting a role of jasmonic acid in *Arabidopsis* leaf senescence. *Plant Physiol.* **2002**, *128*, 876–884. [CrossRef]
- 62. Yoshida, S.; Ito, M.; Nishida, I.; Watanabe, A. Isolation and RNA gel blot analysis of genes that could serve as potential molecular markers for leaf senescence in *Arabidopsis thaliana*. *Plant Cell Physiol*. **2001**, 42, 170–178. [CrossRef] [PubMed]

63. Zhen, X.; Liu, C.; Guo, Y.; Yu, Z.; Han, Y.; Zhang, B.; Liang, Y. Leaf Senescence regulation mechanism based on comparative transcriptome analysis in *Foxtail millet*. *Int. J. Mol. Sci.* **2024**, 25, 3905. [CrossRef] [PubMed]

- 64. Lin, M.; Pang, C.; Fan, S.; Song, M.; Wei, H.; Yu, S. Global analysis of the *Gossypium hirsutum* L. transcriptome during leaf senescence by RNA-Seq. *BMC Plant Biol.* **2015**, *15*, 43. [CrossRef]
- 65. Wu, X.Y.; Hu, W.J.; Luo, H.; Xia, Y.; Zhao, Y.; Wang, L.D.; Zhang, L.M.; Luo, J.C.; Jing, H.C. Transcriptome profiling of developmental leaf senescence in sorghum (*Sorghum bicolor*). *Plant Mol. Biol.* **2016**, 92, 555–580. [CrossRef] [PubMed]
- 66. Sekhon, R.S.; Saski, C.; Kumar, R.; Flinn, B.S.; Luo, F.; Beissinger, T.M.; Ackerman, A.J.; Breitzman, M.W.; Bridges, W.C.; de Leon, N.; et al. Integrated genome-scale analysis identifies novel genes and networks underlying senescence in *maize*. *Plant Cell* 2019, 31, 1968–1989. [CrossRef]
- 67. Zhu, F.; Alseekh, S.; Koper, K.; Tong, H.; Nikoloski, Z.; Naake, T.; Liu, H.; Yan, J.; Brotman, Y.; Wen, W.; et al. Genome-wide association of the metabolic shifts underpinning dark-induced senescence in *Arabidopsis*. *Plant Cell* **2022**, *34*, 557–578. [CrossRef]
- 68. Zhou, L.; Chang, G.; Shen, C.; Teng, W.; He, X.; Zhao, X.; Jing, Y.; Huang, Z.; Tong, Y. Functional divergences of natural variations of TaNAM-A1 in controlling leaf senescence during wheat grain filling. *J. Integr. Plant Biol.* **2024**, *66*, 1242–1260. [CrossRef]
- 69. Saher, S.; Piqueras, A.; Hellin, E.; Olmos, E. Hyperhydricity in micropropagated carnation shoots: The role of oxidative stress. *Physiol. Plant.* **2004**, *120*, 152–161. [CrossRef]
- 70. Young, M.D.; Wakefield, M.J.; Smyth, G.K.; Oshlack, A. Gene ontology analysis for RNA-seq: Accounting for selection bias. *Genome Biol.* **2010**, *11*, R14. [CrossRef]
- 71. Mao, X.; Cai, T.; Olyarchuk, J.G.; Wei, L. Automated genome annotation and pathway identification using the KEGG Orthology (KO) as a controlled vocabulary. *Bioinformatics* **2005**, *21*, 3787–3793. [CrossRef]
- 72. Yin, P.; Ma, Q.; Wang, H.; Feng, D.; Wang, X.; Pei, Y.; Wen, J.; Tadege, M.; Niu, L.; Lin, H. SMALL LEAF AND BUSHY1 controls organ size and lateral branching by modulating the stability of BIG SEEDS1 in *Medicago truncatula*. *New Phytol.* **2020**, 226, 1399–1412. [CrossRef] [PubMed]
- 73. Chen, H.; Zou, Y.; Shang, Y.; Lin, H.; Wang, Y.; Cai, R.; Tang, X.; Zhou, J.M. Firefly luciferase complementation imaging assay for protein-protein interactions in plants. *Plant Physiol.* **2008**, *146*, 368–376. [CrossRef] [PubMed]

Disclaimer/Publisher's Note: The statements, opinions and data contained in all publications are solely those of the individual author(s) and contributor(s) and not of MDPI and/or the editor(s). MDPI and/or the editor(s) disclaim responsibility for any injury to people or property resulting from any ideas, methods, instructions or products referred to in the content.